Supplemental Document

OPTICA QUANTUM

Reconciling quantum and classical spectral theories of ultrastrong coupling: role of cavity bath coupling and gauge corrections: supplement

STEPHEN HUGHES,[1,*] CHRIS GUSTIN,[2] AND FRANCO NORI[3]

[1]*Department of Physics, Engineering Physics and Astronomy, Queen's University, Kingston, ON K7L 3N6, Canada*
[2]*Edward L. Ginzton Laboratory, Stanford University, Stanford, California 94305, USA*
[3]*Theoretical Quantum Physics Laboratory, Cluster for Pioneering Research, RIKEN, Wako-shi, Saitama 351-0198, Japan, Center for Quantum Computing, RIKEN, Wako-shi, Saitama 351-0198, Japan, Physics Department, The University of Michigan, Ann Arbor, Michigan 48109-1040, USA*
[*]*shughes@queensu.ca*

Supplement DOI: https://doi.org/10.6084/m9.figshare.25368586

Parent Article DOI: https://doi.org/10.1364/OPTICAQ.519395

Supplementary Material for "Reconciling quantum and classical spectral theories of ultrastrong coupling: Role of cavity bath coupling and gauge corrections"

Stephen Hughes,[1,*] Chris Gustin,[2,†] and Franco Nori[3,4,5,‡]

[1] *Department of Physics, Engineering Physics and Astronomy, Queen's University, Kingston, ON K7L 3N6, Canada*

[2] *Edward L. Ginzton Laboratory, Stanford University, Stanford, California 94305, USA*†

[3] *Theoretical Quantum Physics Laboratory, Cluster for Pioneering Research, RIKEN, Wako-shi, Saitama 351-0198, Japan*

[4] *Center for Quantum Computing, RIKEN, RIKEN, Wako-shi, Saitama 351-0198, Japan*

[5] *Physics Department, The University of Michigan, Ann Arbor, Michigan 48109-1040, USA*

(Dated: March 1, 2024)

In this supplementary material document, we provide: (i) further details about the classical scattering theory and spectrum, (ii) some technical details on our numerical solution of the master equation, (iii) calculations to show the role of the cavity bath spectral function, (iv) calculations to demonstrate the role of the cavity pump rate (beyond weak excitation), and (v) a derivation of the perturbative Bloch-Siegert regime, to support the numerical findings about the spectral linewidths, and in particular how the classical solution is obtain only when one uses $\Pi_c = \frac{1}{\sqrt{2}}(P \pm Q)$ for the cavity bath operator with gauge corrections.

I. CLASSICAL SCATTERING THEORY AND CLASSICAL SPECTRUM

Here we briefly present the background theory needed to derive the the cavity-emitted classical spectrum shown in the main text. The classical spectrum, at any point $\mathbf{r}$, is obtained from

$$S^{\text{Class}}(\mathbf{r},\omega) = (\mathbf{E}(\mathbf{r},\omega))^* \cdot \mathbf{E}(\mathbf{r},\omega), \tag{1}$$

where $\mathbf{E}(\mathbf{r},\omega)$ is the classical electromagnetic scattered field, which is obtained from solution of a Green function dipole response (at position $\mathbf{r}_0$, polarized along $\mathbf{n}_d$):

$$\mathbf{E}(\mathbf{r},\omega) = \mathbf{G}(\mathbf{r},\mathbf{r}_0,\omega) \cdot \boldsymbol{\alpha}(\omega) \cdot \mathbf{E}_0, \tag{2}$$

where $\mathbf{E}_0$ is the homogeneous field excitation at the dipole location (assumed to be frequency independent), and $\boldsymbol{\alpha}$ is the exact polarizability volume, namely it also contains the coupling to the cavity medium, defined from $\boldsymbol{\alpha}(\omega) = \boldsymbol{\alpha}_0(\omega) + \boldsymbol{\alpha}_0(\omega) \cdot \mathbf{G}(\mathbf{r}_0,\mathbf{r}_0,\omega) \cdot \boldsymbol{\alpha}(\omega)$, where $\boldsymbol{\alpha}_0(\omega) = \alpha_0(\omega)\mathbf{n}_d\mathbf{n}_d^\dagger$ is the bare polarizability (i.e., without radiative coupling to the medium) [1], and $\mathbf{n}_d$ is unit vector (dipole direction). This can easily be derived from a Dyson solution, for the total medium *including* the point dipole emitter [2]. Equivalently, one can use the exact Green function (i.e., with the emitter included), and then work with $\alpha_0(\omega)$, but final results are identical [3].

The classical Green function of the medium, which has units of inverse volume, is defined from

$$\boldsymbol{\nabla} \times \boldsymbol{\nabla} \times \mathbf{G}(\mathbf{r},\mathbf{r}',\omega) - \frac{\omega^2}{c^2}\epsilon(\mathbf{r},\omega)\mathbf{G}(\mathbf{r},\mathbf{r}',\omega) = \frac{\omega^2}{c^2}\mathbb{1}\delta(\mathbf{r}-\mathbf{r}'), \tag{3}$$

where $\epsilon(\mathbf{r},\omega)$ is the dielectric function of the medium which is in general complex, and $\mathbb{1}$ is the unit tensor. For a single mode cavity, the Green function can be defined in terms of the dominant cavity mode, so that

$$\mathbf{G}(\mathbf{r},\mathbf{r}',\omega) = \frac{\mathbf{f}_c(\mathbf{r})\mathbf{f}_c^*(\mathbf{r}')\omega^2}{\omega_c^2 - \omega^2}, \tag{4}$$

and we obtain equations (4) and (5) in the main text, where we also introduced $A_c = |\mathbf{f}_c(\mathbf{r}_0)|^2$. Using the same cavity mode projection for the electric field at the detected location $\mathbf{r}$, we then obtain the classical spectrum in the main text, namely, equation (6), where the geometrical factor depends on the cavity mode strength $\mathbf{f}_c(\mathbf{r})$.

II. NUMERICAL PARAMETERS FOR OUR MASTER EQUATION SIMULATIONS

To solve our generalized master equation (GME), we first adopt a Hilbert space with a basis of 80 harmonic oscillator states and 2 states for the two level atom. For both the quantum Rabi model and the Hopfield model, we then truncate to a combined dressed-state basis of 25 dressed states, and construct and solve the GME in that basis. We solve as a function of time, for times long enough to ensure numerical convergence.

* shughes@queensu.ca
† cgustin@stanford.edu
‡ fnori@riken.jp

III. INFLUENCE OF CAVITY BATH SPECTRAL FUNCTION

Here we also demonstrate the influence of having a more general spectral bath function, $J_c(\omega)$. In Fig. 1 below, we show examples with a flat bath function [(a): $J_c(\omega) \propto \kappa$], as in the main text, and and Ohmic bath function [(b): $J_c(\omega) \propto \kappa\omega/\omega_c$], with $\eta = 0.5$. In the simulations, we use $\Pi_c = \frac{1}{\sqrt{2}}(P+Q)$ as in figure 2(c) of the main text. As might be expected, a non-flat bath has a significant influence on both the spectral asymmetry as well as the linewidths of the spectral resonances.

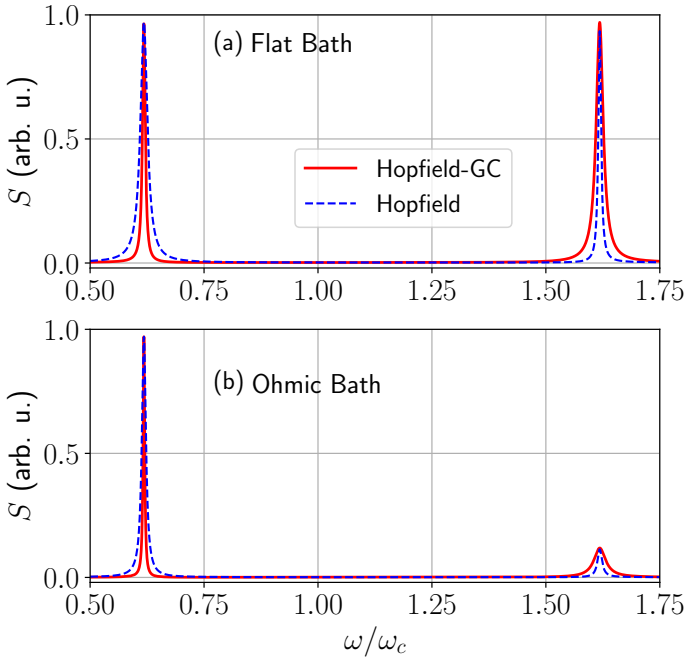

Figure 1. Hopfield master equation results for $\eta = 0.5$, and $\kappa = 0.05g$, using $\Pi_c = \frac{1}{\sqrt{2}}(P+Q)$, with two different spectral bath functions: (a) flat bath, as in the main text, and (b) an Ohmic bath function. Red solid lines show the gauge corrected results, and blue dashed shows uncorrected results (see main text for modle details).

Similar results are obtained for the dissipative quantum Rabi model, as shown in Fig. 2.

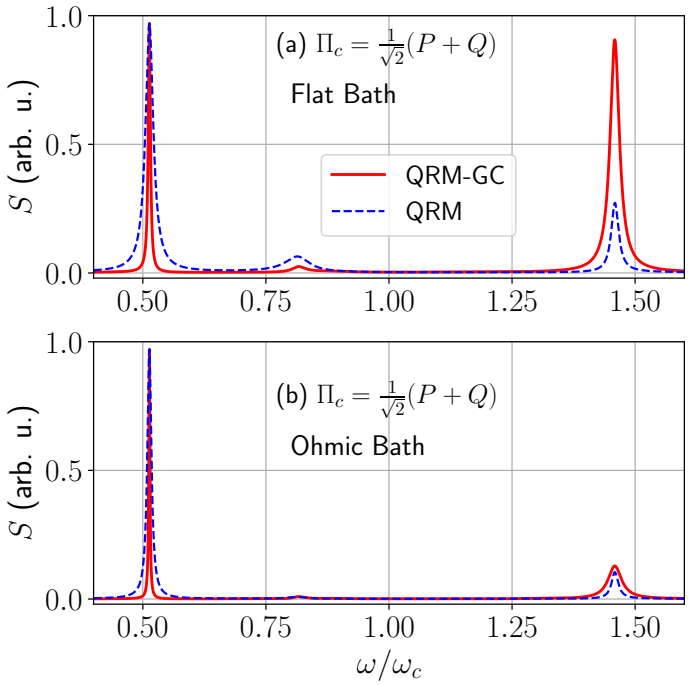

Figure 2. As in Fig. 1, but for the quantum Rabi model (QRM).

IV. INFLUENCE OF CAVITY PUMP RATE

Our quantum theory is not restricted to weak excitations, which was used in the main text to find the equivalence with the linear classical results. After finding this equivalence in the weak-excitation regime, then our model can safely explore larger pumping regimes as well. Here we just show the influence with an increasing cavity pump rate, whose effect is of course related to the specific pump model we use in the quantum model. Similar models have been used to explain nonlinear photoluminescence experiments of excited quantum dot cavity systems in the strong-coupling regime [4, 5].

To appreciate the role of the pump rate beyond weak excitation, we show an example here for the $\eta = 0.5$ case that was also used in Fig. 1 [and figure 2(c) of the main text], but now we show results for three different pumping rates: (a) $P_c = 0.1\kappa$, (b) $P_c = 0.5\kappa$, and (c) $P_c = \kappa$, which demonstrate the significant influence for increasing pump strengths. In particular, larger pump strengths cause additional broadening, that are more notable for the upper polariton, which also has a reduction in oscillator strength. As in the main text, here we use a flat spectral bath function.

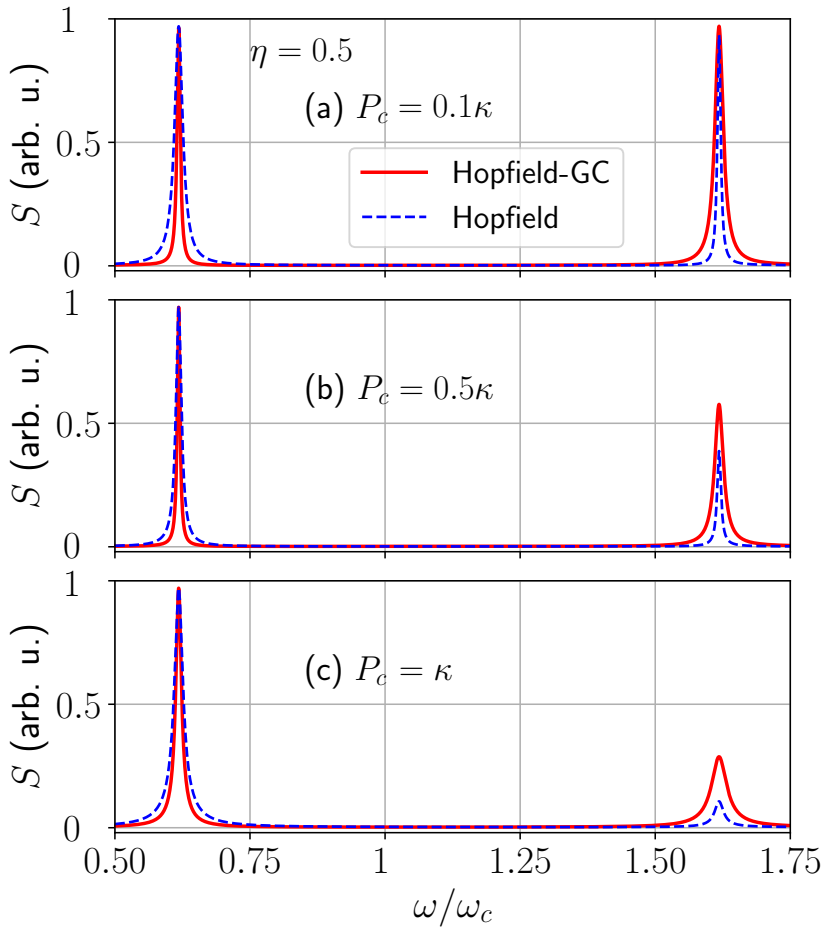

Figure 3. Hopfield master equation results for $\eta = 0.5$, and $\kappa = 0.05g$, using $\Pi_c = \frac{1}{\sqrt{2}}(P + Q)$, with three different cavity pump strengths: (a) $P_c = 0.1\kappa$, (b) $P_c = 0.5\kappa$, and (c) $P_c = \kappa$.

V. PERTURBATIVE BLOCH-SIEGERT REGIME

In this section, we compare the spectral linewidths of the dissipative Hopfield model using both classical and quantum models. To derive analytical results, we limit ourselves to the Bloch-Siegert (BS) regime, where $\eta \sim 0.1$, and we can retain only the lowest order corrections in η.

First, we consider the classical result. To lowest order in both κ (strong-coupling limit), as well as η (Bloch-Siegert regime), we can calculate the complex poles of the classical spectrum given by equation (6) in the main text. The result is (for the upper half-plane poles) $\omega = \omega_\pm + i\frac{\kappa}{2}\alpha_\pm$, where

$$\alpha_\pm = \frac{1}{2}\left[1 \pm \eta\right], \tag{5}$$

with $\omega_\pm$ given by equation (2) in the main text, and we assume $\omega_0 = \omega_c$ from now on.

Next, we compare this result to that of the quantum formalism. Starting from the system Hopfield Hamiltonian in the dipole gauge (equation (1) in the main text), we first perform the Bogoliubov transformation to eliminate the displacement squared term:

$$b = \sqrt{\frac{\chi+1}{2}}\tilde{b} - \sqrt{\frac{\chi-1}{2}}\tilde{b}^\dagger, \tag{6}$$

where

$$\chi = \frac{1+2\eta^2}{\sqrt{1+4\eta^2}}, \tag{7}$$

which satisfies $[\tilde{b}, \tilde{b}^\dagger] = 1$. This leads to

$$H_{\text{Hop}} = \omega_c a^\dagger a + \tilde{\omega}_0 \tilde{b}^\dagger \tilde{b} + i\tilde{g}(a^\dagger - a)(\tilde{b} + \tilde{b}^\dagger), \tag{8}$$

where $\tilde{\omega}_0 = \omega_0 \left[1+4\eta^2\right]^{\frac{1}{2}}$, and $\tilde{g} = g\left[1+4\eta^2\right]^{-\frac{1}{4}}$, and we have dropped a constant term (specifically, $D = \eta g$).

Next, we introduce the BS transformation defined by unitary operator

$$U_{\text{BS}} = \exp\left[-i\frac{\eta}{2}\left(a\tilde{b} + a^\dagger\tilde{b}^\dagger\right)\right], \tag{9}$$

which eliminates the counter-rotating terms to leading order in η. Retaining terms in the Hamiltonian of order η^2 at most, this gives

$$U_{\text{BS}}^\dagger H_{\text{Hop}} U_{\text{BS}} = \omega_0\left(1+\frac{3}{2}\eta^2\right)\tilde{b}^\dagger\tilde{b} + \omega_0\left(1-\frac{\eta^2}{2}\right)a^\dagger a + ig\left(a^\dagger\tilde{b} - a\tilde{b}^\dagger\right) + V_2, \tag{10}$$

where $V_2 = \frac{g^2}{2\omega_0}\left(a^2 + a^{\dagger 2} - \tilde{b}^2 - \tilde{b}^{\dagger 2}\right)$ can be removed by an additional unitary transformation which introduces no other changes to leading order—we thus neglect it going forward [6]. From here, we can verify (i.e., from calculating the energy of the lowest two excited states) that the resonances are, to order η^2, $\omega_\pm = \omega_0\left[1 + \frac{\eta^2}{2} \pm \eta\right]$, in agreement with the exact Bogoliubov solution in the main text, as expected. To leading order in η, the lowest energy corrected Jaynes-Cummings–like excited eigenstates are

$$|\pm\rangle = \frac{i}{\sqrt{2}}\left(1 \mp \frac{\eta}{2}\right)a^\dagger|0\rangle + \frac{1}{\sqrt{2}}\left(\pm 1 + \frac{\eta}{2}\right)\tilde{b}^\dagger|0\rangle \tag{11}$$

With this, we can calculate the linewidths of the weak-excitation spectra, following the derivation in Ref. [7]. For the system operator Π_c which couples to the reservoir, we consider the generic form

$$\Pi_c(\theta) = \cos\theta Q + \sin\theta P, \tag{12}$$

where $Q = a + a^\dagger$, and $P = i(a^\dagger - a)$. We first consider the case with no gauge corrections. Under the BS transformation (denoting transformed variables with primes), we then have

$$\Pi_c'(\theta) = \cos\theta\left[Q + i\frac{\eta}{2}(\tilde{b} - \tilde{b}^\dagger)\right] + \sin\theta\left[P - \frac{\eta}{2}(\tilde{b} + \tilde{b}^\dagger)\right], \tag{13}$$

and following Ref. [7], the linewidths for well-separated peaks in the weak-excitation limit are, to order η,

$$\Gamma_\pm(\theta) = \kappa\left|\langle 0|\Pi_c'(\theta)|\pm\rangle\right|^2 = \frac{\kappa}{2}\left[1 \mp 2\eta\sin^2(\theta)\right]. \tag{14}$$

Clearly, we see that, without considering gauge corrections due to the single-mode model for the polariton system, there is *no possible system operator* $\Pi'(\theta)$ that can recover the classical result in Eq. (5).

With gauge corrections, we have $Q \to Q$, and $P \to P + 2\eta(\tilde{b} + \tilde{b}^\dagger)$, so in the BS frame we have

$$\Pi_{\text{c,GC}}'(\theta) = \cos\theta\left[Q + i\frac{\eta}{2}(\tilde{b} - \tilde{b}^\dagger)\right] + \sin\theta\left[P + \frac{3}{2}\eta(\tilde{b} + \tilde{b}^\dagger)\right], \tag{15}$$

and so,

$$\Gamma_\pm^{\text{GC}}(\theta) = 2\kappa\left|\langle 0|\Pi_{\text{c,GC}}'(\theta)|\pm\rangle\right|^2 = \frac{\kappa}{2}\left[1 \pm 2\eta\sin^2(\theta)\right]. \tag{16}$$

Clearly, only $\theta = \pm\frac{\pi}{4}$ gives agreement with the classical result of Eq. (5), shown above, which corresponds to $\Pi_c = \frac{1}{\sqrt{2}}[P \pm Q]$.

For completeness we can also carry out this calculation for the QRM. The result is a simple generalization of that from Ref. [7], and gives

$$\Gamma_{\pm}^{\mathrm{QRM}}(\theta) = \frac{\kappa}{2}\left[1 \pm \eta\left(\frac{1}{2} - 2\sin^2(\theta)\right)\right], \tag{17}$$

without gauge corrections, and

$$\Gamma_{\pm}^{\mathrm{GC,QRM}}(\theta) = \frac{\kappa}{2}\left[1 \pm \eta\left(\frac{1}{2} + 2\sin^2(\theta)\right)\right] \tag{18}$$

with gauge corrections. Letting $\theta = \pi/2$ recovers the result from Ref. [7],

[1] P. de Vries, D. V. van Coevorden, and A. Lagendijk, Point scatterers for classical waves, Rev. Mod. Phys. **70**, 447 (1998).

[2] C. P. Van Vlack, *Dyadic Green Functions and their Applications*, Ph.D. thesis, Queen's University, Canada (2012).

[3] P. T. Kristensen, J. Mørk, P. Lodahl, and S. Hughes, Decay dynamics of radiatively coupled quantum dots in photonic crystal slabs, Phys. Rev. B **83**, 075305 (2011).

[4] A. Laucht, N. Hauke, J. M. Villas-Bôas, F. Hofbauer, G. Böhm, M. Kaniber, and J. J. Finley, Dephasing of exciton polaritons in photoexcited ingaas quantum dots in gaas nanocavities, Phys. Rev. Lett. **103**, 087405 (2009).

[5] P. Yao, P. K. Pathak, E. Illes, S. Hughes, S. Münch, S. Reitzenstein, P. Franeck, A. Löffler, T. Heindel, S. Höfling, L. Worschech, and A. Forchel, Nonlinear photoluminescence spectra from a quantum-dot–cavity system: Interplay of pump-induced stimulated emission and anharmonic cavity QED, Phys. Rev. B **81**, 033309 (2010).

[6] A. Le Boité, Theoretical methods for ultrastrong light–matter interactions, Adv. Quantum Technol. **3**, 1900140 (2020).

[7] W. Salmon, C. Gustin, A. Settineri, O. D. Stefano, D. Zueco, S. Savasta, F. Nori, and S. Hughes, Gauge-independent emission spectra and quantum correlations in the ultrastrong coupling regime of open system cavity-QED, Nanophotonics **11**, 1573 (2022).